Topographic effects for incident P, SV and Rayleigh waves

Francisco J. Sánchez-Sesma [a,b] and Michel Campillo [c]

[a] *Instituto de Ingeniería, UNAM Cd. Universitaria, Apdo. 70-472, Coyoacán 04510, México D.F., Mexico*
[b] *Centro de Investigación Sísmica, A.C. Carr. al Ajusco 203, Col. H. de Padierna, Tlalpan 14200, México D.F., Mexico*
[c] *Observatoire de Grenoble, Université Joseph Fourier, LGIT-IRIGM, BP 53X, 38041 Grenoble Cedex, France*

ABSTRACT

Sánchez-Sesma, F.J. and Campillo, M., 1993. Topographic effects for incident P, SV and Rayleigh waves. In: F. Lund (Editor), New Horizons in Strong Motion: Seismic Studies and Engineering Practice. *Tectonophysics*, 218: 113–125.

The topographical effects for incident P, SV and Rayleigh waves in an elastic half-space were studied using an integral representation of the diffracted elastic waves in terms of single-layer boundary sources. The free-boundary condition leads to a Fredholm integral equation of the second kind for boundary sources. We used a discretization scheme based on the numerical and analytical integration of exact Green's functions. This approach is called indirect BEM in the literature. However, it provides far more insight on the physics of diffraction problems than the direct approaches. This is because diffracted waves are constructed at the boundaries from which they are radiated. Therefore, this method can be regarded as a numerical realization of Huygens' principle. Various examples that cover extreme cases are presented. It is found that topography may cause significant effects both of amplification and of deamplification at the irregular feature itself and its neighborhood but the absolute level of amplification is generally lower than about 4 times the amplitude of incoming waves. These facts must be taken into account when the spectral ratio technique is used to study topographical response.

Introduction

The effects of local site conditions may produce large ground motion amplification during earthquakes and concentrated damage (see Sánchez-Sesma (1987) and Aki (1988) for reviews). During the last two decades significant progress has been achieved both in the observation and in the evaluation of such effects. In particular, the effects of topography on surface ground motion have been observed and studied from field experiments. Trifunac and Hudson (1971), Davis and West (1973), Griffiths and Bollinger (1979) and Tucker et al. (1984), among others, discovered significant effects. However, as pointed out by Bard and Tucker (1985) and Geli

et al. (1988), the observed amplifications in the field are systematically larger than the values predicted using theoretical models (e.g., Bard, 1982). They suggested that the models should incorporate layering, variations in wave velocities and even irregular two- and three-dimensional configurations in order to explain the observations more precisely. Bard and Tucker (1985) have tested several such models and improved the predictions but still showed amplifications smaller than the observed ones.

Theoretical studies aimed at predicting site effects are numerous. It is worth mentioning the work by Trifunac (1971; 1973), who found analytical solutions for the response of semi-circular alluvial valleys and canyons under incident SH waves. Other analytical solutions have been recently obtained for shallow circular geometries (e.g. Lee and Cao, 1989; Todorovska and Lee, 1992a,b). An exact solution for the incidence of plane SH and SV waves upon an infinite, moun-

Correspondence to: F.J. Sánchez-Sesma, Instituto de Ingeniería, UNAM Cd. Universitaria, Apdo. 70-472, Coyoacán 04510, Mexico D.F., Mexico.

tain-like wedge has been obtained for certain angles by geometrical means (Sánchez-Sesma, 1990). For arbitrary geometries analytical solutions are no longer valid. Therefore, numerical techniques have to be developed. A recent compilation of works on the numerical modeling of seismic wave propagation in realistic media (Kelly and Marfurt, 1990) gives a good account of the state-of-the-art of the so-called domain methods.

Boundary methods have gained increasing popularity. The boundary integral equation (BIE) and their discretizations into boundary element methods (BEM) have been useful in the study of dynamic elasticity problems. Among the advantages over domain approaches are the dimensionality reduction and the simple fulfillment of radiation conditions at infinity. Excellent surveys of the available literature on BEM in elastodynamics are those of Kobayashi (1987) and Manolis and Beskos (1988). The most popular BEM approaches are the so-called *direct*, because in their formulation the unknowns are the sought values of displacements and tractions. They arise from the discretization of integral representation theorems. It is worth noting that Wong and Jennings (1975) used a direct formulation based on an integral representation to study the seismic response of arbitrary canyon geometries. A similar approach was used by Zhang and Chopra (1991) to consider the three-dimensional response of canyons.

In contrast, the *indirect* BEM, which formulates the problem in terms of force or moment boundary densities, is not as popular. This is despite the fact that such densities can give a deep physical insight into the nature of diffracted waves. Moreover, the indirect BEM has a longer history than the direct BEM and is closely related to classical work on integral equations (see, for example, Manolis and Beskos, 1988).

On the other hand, the combination of discrete wavenumber expansions for Green's functions (Bouchon and Aki, 1977; Bouchon, 1979) with boundary integral representations has been successful in various studies of elastic wave propagation. Bouchon (1985), Campillo and Bouchon (1985), Campillo (1987), Gaffet and Bouchon (1989), Bouchon et al. (1989) and Campillo et al.

(1990) used source distributions on the boundaries, whereas Kawase (1988) and Kawase and Aki (1989) used Somigliana representation theorem. These two approaches are discrete wavenumber versions of indirect BEM and direct BEM, respectively. However, such procedures require a considerable amount of computer resources. An alternative approach may be welcomed for many applications.

In this work we study the surface motion at various topographic features for incident P, SV and Rayleigh waves. This plane strain case can be regarded as the simplest of a class of vector problems of seismological interest. We use a single-layer boundary integral representation of diffracted waves. Therefore, our method can be classified as an indirect BEM. In this approach, diffracted waves are constructed at the boundaries from which they are radiated. Therefore, it can be regarded as a numerical realization of Huygens' principle (this is true for any indirect method). This approach is, in fact, an improvement over the boundary method, which has been used to deal with various problems of the diffraction of elastic waves (see, for example, Sánchez-Sesma and Esquivel, 1979; Sánchez-Sesma and Rosenblueth, 1979; Dravinski, 1982; Wong, 1982; Dravinski and Mossessian, 1987; Luco et al., 1990). In its many variants, such a technique is based upon the superposition of solutions for sources with their singularities placed outside the region of interest. However, this requires particular care and the trial and error process needed is difficult to apply, particularly when many frequencies are to be computed.

As the singularities of Green's functions are integrable (e.g., Kobayashi, 1987; Manolis and Beskos, 1988) we can put the sources at the boundary and properly consider their effects. In this way, the uncertainty about the location of sources is eliminated and the linear system of equations that arises from the discretization can be directly solved. Therefore, our indirect BEM approach retains the physical insight of the sources method, with all the benefits of the analytical integration of exact Green's functions. In the applications reported here, we represent diffracted fields with the superposition of the

radiation from boundary sources using exact expressions of the two-dimensional Green's functions in an unbounded elastic space.

In order to test the method, we compared results with those obtained by Wong (1982), Sánchez-Sesma et al. (1985) and Kawase (1988) for the incidence of P, SV and Rayleigh waves upon a semi-circular canyon on a half-space. We found excellent agreement with those results. Moreover, we present various examples that cover extreme profiles. We show that relatively simple topographies may induce significant variations in the ground motion at and around the irregularity. We believe that this fact partially explains the large relative amplifications reported in the literature (e.g., Geli et al., 1988). Our examples show that, even though relative amplification due to the topography is sometimes quite big, the absolute level of amplification is generally lower than about 4 times the amplitude of incoming waves. Such facts must be taken into account when the spectral ratio technique is used to characterize topographic effects.

Integral representation using boundary sources

Consider the domain, V and its boundary, S. If an elastic material occupies such a region, the displacement field under harmonic excitation can be written (neglecting body forces) by means of the single layer boundary integral:

$$u_i(x) = \int_S \phi(\xi) G_{ij}(x,\xi) \, dS_\xi \qquad (1)$$

where $u_i(x) = i$th component of displacement at x; $G_{ij}(x,\xi)$ = Green function, that is, the displacement in the direction i at point x, due to the application of a unit force in the direction j at point ξ; $\phi_j(\xi)$ = force density in the direction j. Therefore, $\phi_j(\xi) dS$ is clearly a force distribution at the boundary. The subscripts in the differentials indicate the space variable over which the integration is performed.

This single layer integral, which can be related to Somigliana identity (Sánchez-Sesma and Campillo, 1991), has been studied by Kupradze (1963). He showed that the displacement field is continuous across S if $\phi_j(\xi)$ is continuous along S.

This integral representation allows computation of stresses and tractions by direct application of Hooke's law, except at boundary singularities, that is, when $x = \xi$ on the boundary. By a limiting process based on equilibrium considerations around an internal neighborhood of the boundary, it is possible to write, for x on S that:

$$t_i(x) = \tfrac{1}{2}\phi_i(x) + \int_S \phi_j(x) T_{ij}(x,\xi) \, dS_\xi \qquad (2)$$

where $t_i = i$th component of traction at the boundary; $T_{ij}(x,\xi)$ = traction Green function, that is, the traction in the direction i at point x on the boundary with normal, $n(x)$ (assumed to be specified) due to the application of a unit force in the direction j applied at ξ. The first term of the right hand side must be dropped if x is at V. This result was also found by Kupradze (1963). He used a formal technique of singularity extraction, which is now used to deal with the hypersingular integral equations of dynamic elasticity (e.g., Bonnet, 1986; 1989).

Equations (1) and (2) are the basis of our approach. Although *indirect*, it allows direct interpretation of the physical quantities involved. Expressions for Green's functions can be found in the literature (e.g., Kobayashi, 1987; Sánchez-Sesma and Campillo, 1991). It suffices to say here that the singularity of displacements is either logarithmic or $1/r$ for two-dimensional or three-dimensional problems, respectively. Regarding the tractions, such singularities are explicitly of the form $1/r$ or $1/r^2$, respectively. In particular, when the frequency tends to zero, Green's functions lead to their static counterparts. These properties are invoked below in connection with our discretization scheme.

Diffraction of elastic waves by topography

Consider an elastic half space with a localized topographic relief as shown in Figure 1. The ground motion in this irregular configuration comes from the interferences of incoming waves with reflected and diffracted ones. It is also usual to say that the total motion is the superposition of the so-called *diffracted* waves and the free-field:

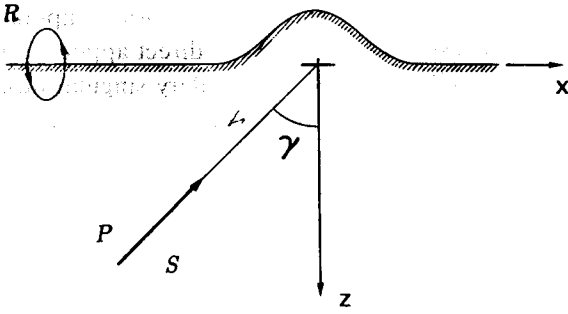$$u_i = u_i^{(0)} + u_i^{(d)} \qquad (3)$$

Fig. 1. Irregular half-space and incidence of P, SV and Rayleigh waves.

where $u_i^{(0)}$ = free-field displacement; that is, the solution in the absence of the irregularity.

In this application the displacement free-field is that produced by incident plane waves and is analytically extended to the parts of the topography that are not included in the reference half-space. This means that incoming and reflected waves are assumed to exist for $z < 0$, fulfilling the same analytical expressions (Navier equations) they satisfy for $z \geqslant 0$. Therefore, the free-field is continuous everywhere.

According to our previous discussion, the diffracted field is given by eqn. (1), which can be written as:

$$u_i^{(d)}(x) = \int_S \phi_j(\xi)G_{ij}(x,\xi)\,dS_\xi \qquad (4)$$

The traction-free boundary condition implies that:

$$t_i^{(0)} + t_i^{(d)} = 0 \qquad (5)$$

then, from eqn. (2), such conditions can be expressed by means of:

$$\tfrac{1}{2}\phi_i(x) + \int_S \phi_j(\xi)T_{ij}(x,\xi)\,dS = -t_i^{(0)} \qquad (6)$$

which is a Fredholm integral equation of the second kind for the boundary tractions; that is, those producing the diffracted field. This expression is discretized along a finite portion of the boundary, S, which includes the topography and the lateral flat parts. We have used values of $3L$–$5L$ (where L = surface length of the surface anomaly). Assuming $\phi_j(\xi)$ is constant over each of the N boundary segments with equal length ΔS, leads to the system of linear equations:

$$\sum_{l=1}^{N} \phi_j(\xi_l)t_{ij}(x_n,\xi_l) = -t_i^{(0)} \quad n = 1,N \qquad (7)$$

where:

$$t_{ij}(x_n,\xi_1) = \tfrac{1}{2}\delta_{ij}\delta_{nl} + \int_{\xi_l - \Delta S/2}^{\xi_l + \Delta S/2} T_{ij}(x_n,\xi)\,dS_\xi \qquad (8)$$

These integrals are computed numerically using Gaussian integration except when $n = l$. In this case we have:

$$t_{ij}(x_n,\xi_n) = \tfrac{1}{2}\delta_{ij} \qquad (9)$$

because the integral in eqn. (8) for $n = l$ is zero as long as the discretization segment is a straight line, which is the case assumed here. It can be verified that, under this circumstance, the integrand is a singular odd function on the segment. Therefore, its Cauchy's principal value is zero. The value for t_{ij} in eqn. (9) can be interpreted as half of the applied unit line force and means that the force is distributed symmetrically for any two half-spaces containing the line of application of the load, regardless of its direction. This result also corresponds to the static solution. Once the values of $\phi_j(\xi_l)$ are known, the diffracted field is computed by means of:

$$u_i^{(d)} = \sum_{l=1}^{N} \phi_j(\xi_l) g_{ij}(x,\xi_l) \qquad (10)$$

where:

$$g_{ij}(x,\xi_l) = \int_{\xi_l - \Delta S/2}^{\xi_l + \Delta S/2} G_{ij}(x,\xi)\,dS_\xi \qquad (11)$$

These integrals are also computed numerically with Gaussian integration, except in the case when x is in the neighborhood of ξ_l, for which we obtained analytical expressions from the ascending series for Bessel functions (e.g., Abramowitz and Stegun, 1972). Sánchez-Sesma and Campillo (1991) presented an example for such expressions when only the leading terms of the series are retained. We considered up to quadratic terms, which is enough if the number of segment per wavelength is larger than about 6. For the elevated portions of the relief the analytical extension of the free-field provides the boundary excitation. In the case of incident Rayleigh waves, or for SV waves with an incidence angle larger than the critical one, the analytical extension gives exponential growth of the extended field (the incident plane SV waves, with an incident angle

of 45°, having no mode conversion and unit re-
flection coefficient, do not present this effect). To
avoid this difficulty we choose to produce
Rayleigh waves by loading our irregular half-space
with a vertical force (e.g., Sánchez-Sesma and
Campillo, 1991). In this case, the excitation comes
from imposing vertical tractions in a small region
of the flat part of the free surface. This illustrates
well the wide potential applications of our
method. The surface load problem is well known
(Lamb, 1904). In this case, more than two-thirds
of the total energy is radiated as Rayleigh waves
(Woods, 1968). At the surface the relative amount
of Rayleigh waves is much larger.

Testing of the method and discussion

The accuracy of this approach has been gauged
by comparing results with those obtained by Wong
(1979; 1982), Sánchez-Sesma et al. (1985) and
Kawase (1988). The diffraction of P, SV and
Rayleigh waves by a semicircular canyon has been
studied by Wong (1979; 1982) for a half-space
with Poisson ratio of 1/3 and no attenuation
using a boundary method. Wong's (1982) results
were verified by Sánchez-Sesma et al. (1985) and
Dravinski and Mossessian (1987), for a normal-
ized frequency $\eta = 0.5$, where $\eta = \omega a / \pi \beta$ and
a = radius of canyon. In general, excellent agree-
ment was found for incident P and SV waves.
The larger difference occurs for Rayleigh waves
in the horizontal motion at the top of the rim of
the canyon: Wong (1982) predicted an amplifica-
tion of about 2.5 there, whereas Sánchez-Sesma
et al. (1985) gave a value of about 2. Figure 2
shows their results, together with our solution.

For a larger normalized frequency, $\eta = 2$ re-
sults by Wong (1982) and Kawase (1988) are
available for Rayleigh waves and for P and SV
waves with an angle of incidence of 0°. Kawase
(1988) used a boundary integral representation
combined with the discrete wavenumber method.
Sánchez-Sesma and Campillo (1991) compared
results for incident P and SV waves. Here we
restrict our comparisons to Rayleigh waves. Fig-
ure 3 shows our results for both horizontal and
vertical displacement amplitudes. We considered
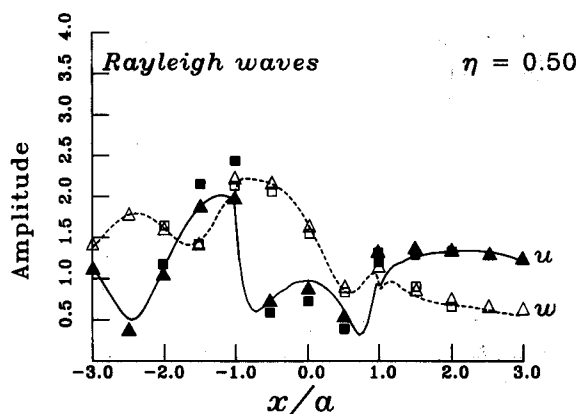a total discretization length of $5L$, where $L = \pi a$,

Fig. 2. Amplitudes of horizontal and vertical displacements
for incidence of harmonic Rayleigh waves upon a semi-cir-
cular canyon. Poisson ratio is 1/3 and the normalized fre-
quency $\eta = 0.5$. Solid and dashed lines = horizontal, u, and
vertical, w, components obtained in this study; squares =
results of Wong (1982); triangles = results of Sánchez-Sesma
et al. (1985).

and 15 segments per S wavelength. The solution
is stable, even when such parameters are reduced
to $3L$ and to 6, respectively. Wong's and Kawase's
results are also shown. Excellent agreement is
found for both horizontal and vertical compo-
nents. However, small differences can be seen.
For instance, both Wong (1982) and Kawase
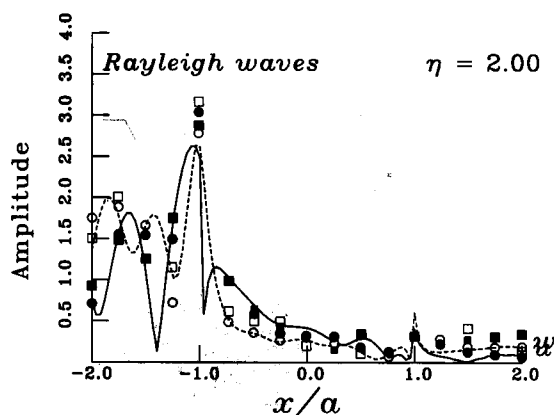(1988) predict amplitudes at the "incidence" rim

Fig. 3. Amplitudes of horizontal and vertical displacements
for incidence of harmonic Rayleigh waves upon a semi-cir-
cular canyon. Poisson ratio is 1/3 and the normalized fre-
quency $\eta = 2$. Solid and dashed lines correspond to horizon-
tal, u, and vertical, w, components obtained in this study;
circles = results of Wong (1982); squares = results of Kawase
(1988).

of the canyon that are somewhat larger than our results. Generally, our results (see also Sánchez-Sesma and Campillo, 1991) are closer to Kawase's. However, in some cases they approach those of Wong. For some locations, both inside and outside the canyon, our results are between the other two results.

These methods are approximate. The only way to assess on their performance is through comparisons of results and with other procedures and by comparing the assumptions and the characteristics of each one. Sánchez-Sesma and Campillo (1991) discussed these issues in detail. Here we will give a brief account.

Both Wong (1982) and Kawase (1988) took as their departure point Lamb's (1904) integrals for the half-space in frequency domain. Wong (1982)

computed such integrals for compressional and shear line sources and used them as trial functions with the singularities "removed from the region of interest"; that is, outside the irregular half-space, inside the region left by the canyon. He satisfied boundary conditions using a generalized inversion scheme, which guarantees good results in a global sense. In contrast, Kawase (1988) integrated analytically along the boundary the expressions of the discrete wavenumber expansion, for which he assumed a horizontal periodicity of ten times the diameter of the canyon. In order to obtain reliable results in the frequency domain, Kawase first got time series and then computed the frequency response. These two methods have the shortcoming of the time-consuming evaluation of Lamb's integrals. Wong
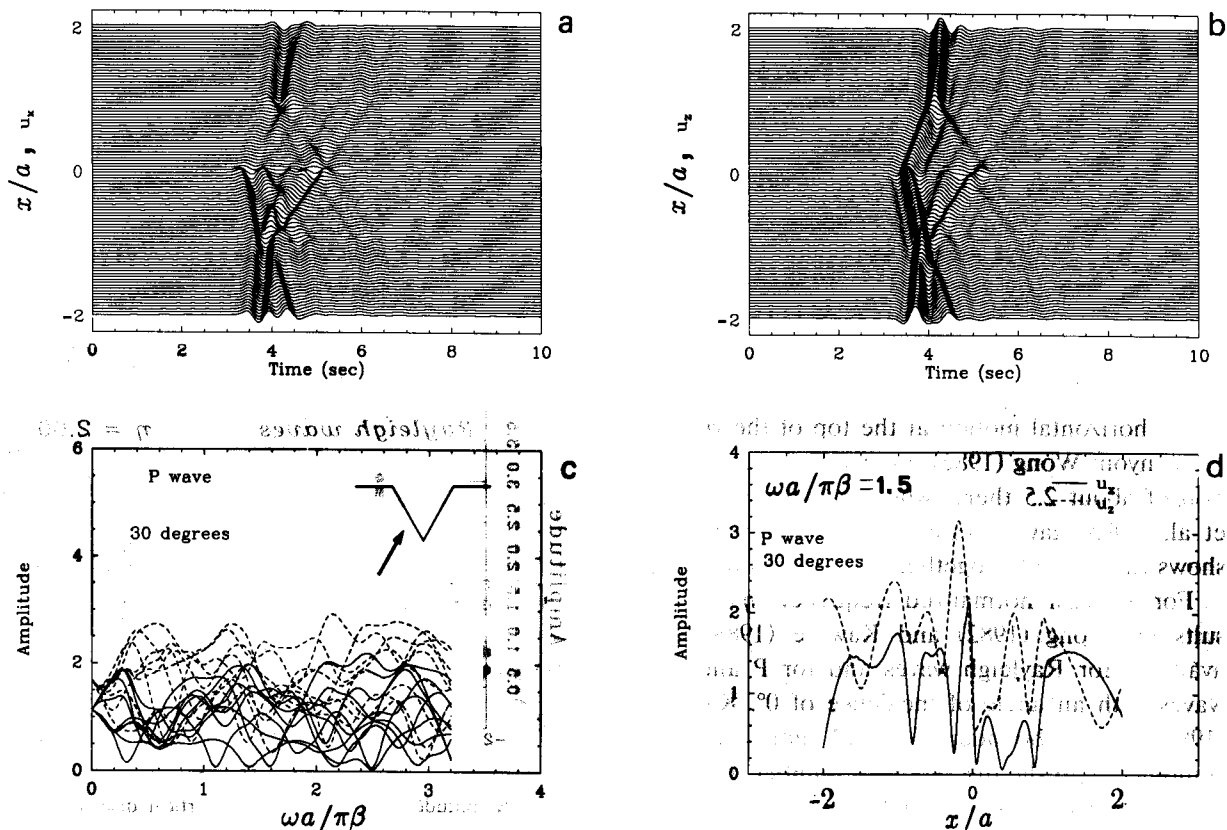

Fig. 4. Incidence of a plane P wave with incidence angle of 30°. Synthetic seismograms and frequency response for surface receivers equally spaced between $x = -2a$ and $x = 2a$ at the surface of a triangular canyon with a angle of dip of 60°. (a) Horizontal component, u_x, and (b) vertical component, u_z. The incident time signal is a Ricker wavelet with central frequency $\omega_p = 1.5\pi\beta/a$. Amplitudes of horizontal (continuous line) and vertical (dotted line) surface displacements (c) for nine receivers against normalized frequency and (d) for the central frequency of the Ricker wavelet for all the receivers against their horizontal location.

(1982), as well as Sánchez-Sesma and Rosen-blueth (1979) for instance, had to accept a certain uncertainty about the optimum location and number of sources.

In contrast, we had less sources of error. We used the exact Green's function for the whole space, which can be computed in a fast manner. Our approach is aimed at obtaining only diffracted waves; that is, those produced both at the irregular boundary and at the free surface, by means of boundary force densities, for which we obtained either exact or analytical values at singularities. Hence, this formulation can be seen as an approximate numerical realization of Huygens' principle (this is true for any indirect formulation). For the numerical integration we used Gaussian integration of three points per segment.

To examine edge effects due to the finite size of the discretized boundary we performed several tests and found that, for the range of frequencies studied, it suffices to discretize a total length of $3L$, where L is the surface length of the topographic feature. The comparisons presented here have been computed for total discretization lengths of $3L$ and $5L$ and the results are virtually the same. This implies that edge effects have little or no influence in our computations and shows that only the discretization of a relatively small part of the free boundary is needed. We consider this fact to be a significant advantage of our approach. Sánchez-Sesma and Campillo (1991) verified this interpretation. They computed the phase of diffracted waves and observed that, for both components, the phase variation with space shows slopes consistent with the expected outgoing nature of such waves.
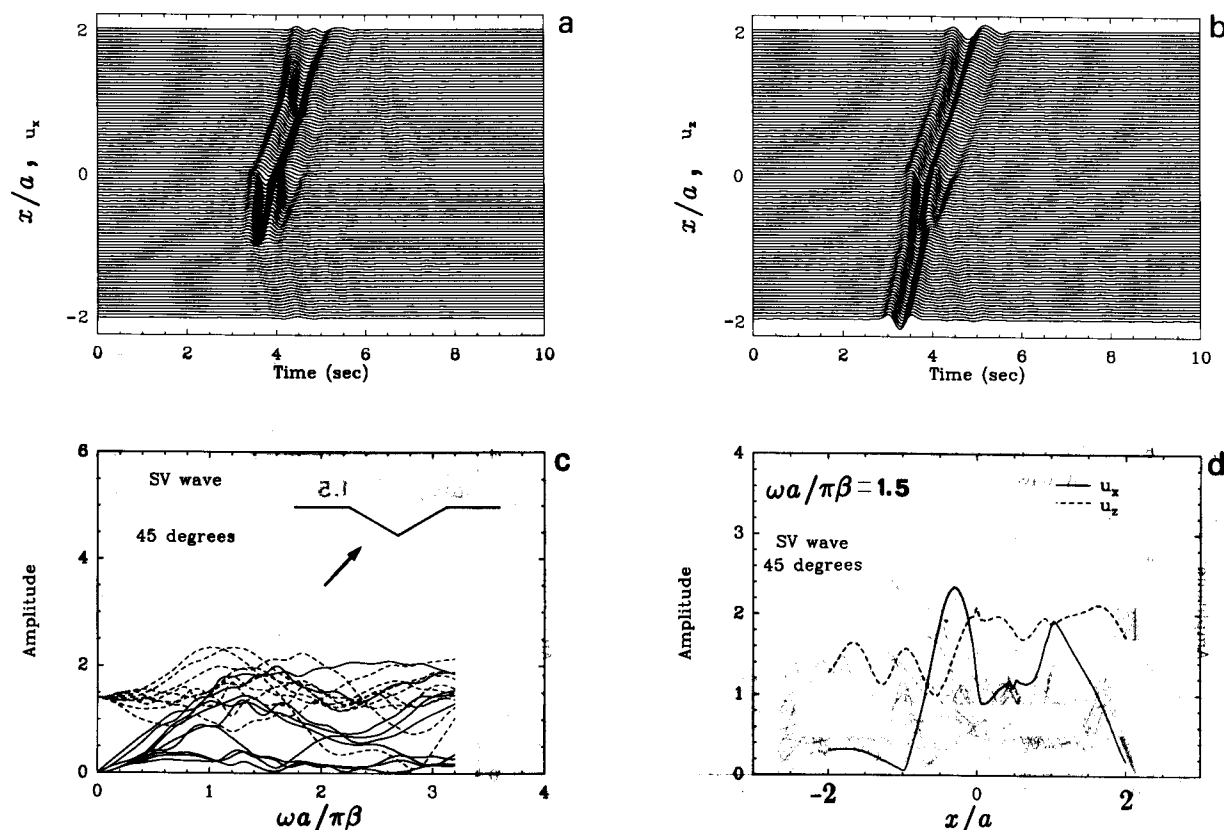

Fig. 5. Incidence of a plane SV wave with incidence angle of 45°. Synthetic seismograms and frequency response for surface receivers equally spaced between $x = -2a$ and $x = 2a$ at the surface of a triangular canyon with an angle of dip of 30°. (a)–(d) as in Fig. 4.

Examples

In order to show the range of effects caused by topography, we present various examples that cover extreme geometries. We choose from a big set of results a sample that, being of reasonable dimension, allows the salient characteristics of such effects to be described. Other examples can be seen in Sánchez-Sesma and Campillo (1991). Our results are displayed in both frequency and time domains for various canyons and mountains under incident P, SV and Rayleigh waves. A Poisson coefficient of 1/4 was selected and no attenuation was assumed. We present five examples:

(1) A triangular canyon with $h = 1.732\,a$, where a = surface half-width (angle of dip 60°) under incident P waves with an angle of incidence of 30° (Fig. 4).

(2) A triangular canyon with $h = 0.577\,a$, where a = surface half-width (angle of dip 30°) under incident SV waves with an angle of incidence of 45° (Fig. 5).

(3) A semi-elliptical canyon with a maximum depth of 3 times the half width ($h = 3a$) under incident SV waves with an angle of incidence of 45° (Fig. 6).

(4) A triangular mountain with an angles of dip of 45° for incident Rayleigh waves (Fig. 7).

(5) A semi-elliptical mountain with a maximum height of $2a$ under incident SV waves with an angle of incidence of 30° (Fig. 8).

For these examples the discretization was carried out over a total length of $3L$, where L = surface length of the topographic feature. The relatively small size of the discretized region is an advantage of our formulation. We used 15 segments per S wavelength.
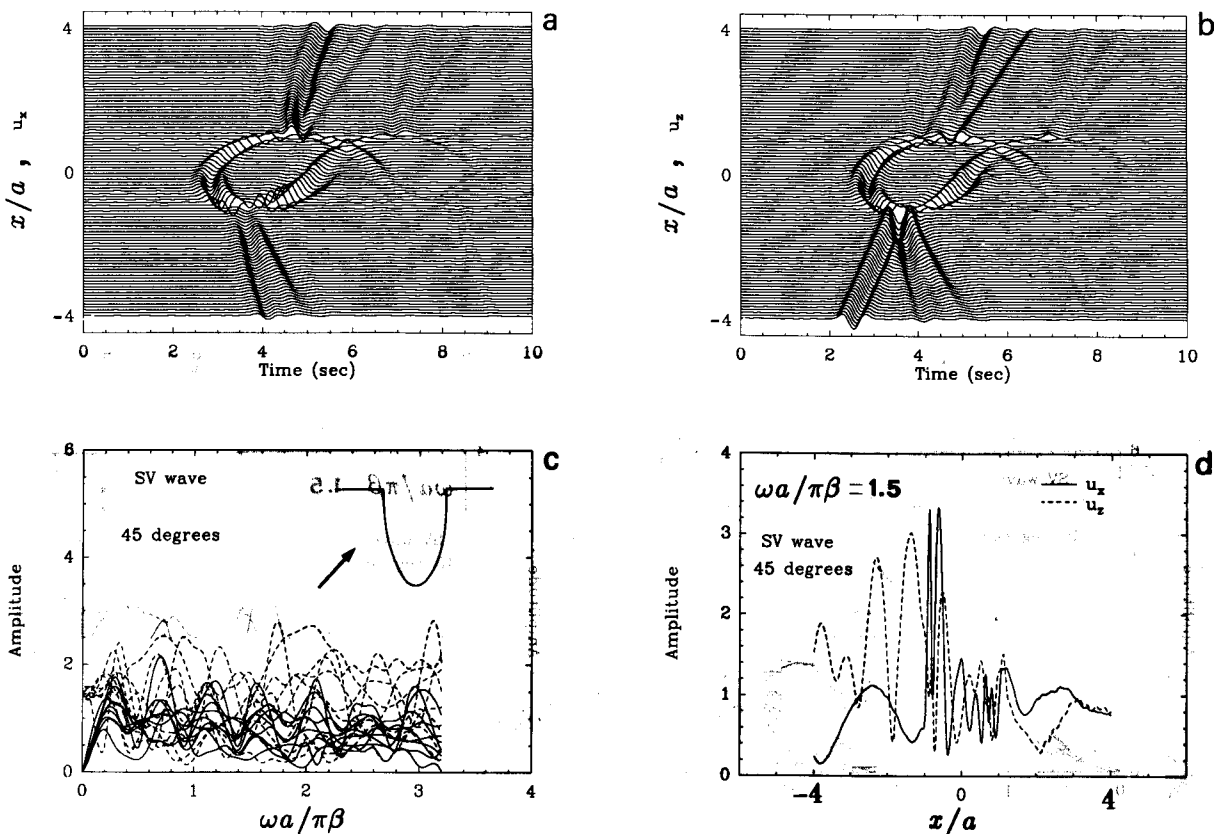

Fig. 6. Incidence of a plane SV wave with incidence angle of 45°. Synthetic seismograms and frequency response for surface receivers equally spaced between $x = -4a$ and $x = 4a$ at the surface of a semi-elliptical canyon with maximum depth of $3a$. (a)–(d) as in Fig. 4.
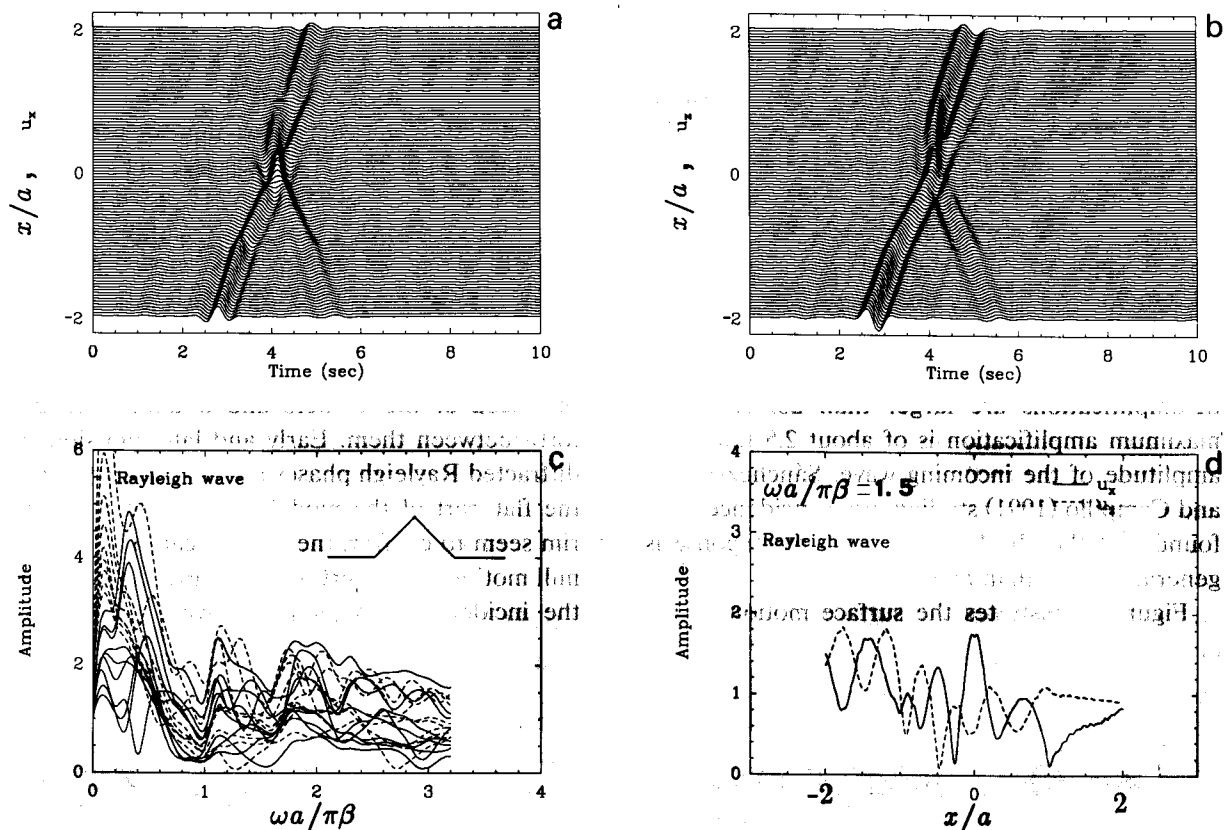
Fig. 8. Incidence of a plane SV wave with incidence angle of 30°. Synthetic seismograms and frequency response for surface receivers equally spaced between $x = -4a$ and $x = 4a$ at the surface of a semi-elliptical mountain with maximum height of $2a$.
(a)–(d) as in Fig. 4.

Results are displayed in Figures 4–8. Each figure contains four plots: synthetic seismograms for horizontal and vertical components, frequency response for selected receivers and spatial variation at a given frequency. Computations were performed in the frequency domain and synthetic seismograms where computed using the FFT algorithm for a Ricker wavelet with central frequency $\omega_p = 1.5\pi\beta/a$ for 101 receivers equally spaced between $x = -4a$ and $x = 4a$ for the semi-elliptical profiles and between $x = -2a$ and $x = 2a$ for the triangular ones. It was assumed that $2a/\beta = 1$ s in order to define the time scale. The actual scale is $\beta t/2a$. The results in the frequency domain are presented against $\omega a/\pi\beta$ and correspond to nine equally spaced surface receivers (out of the 101 for which we computed the synthetics). For the frequency corresponding to the central one of the Ricker pulse, we dis-

played the amplitude of both horizontal and vertical displacements against space.

For the triangular mountain the incident Rayleigh wave is generated with a uniform vertical load applied over a length of $0.25a$ centered at $x = -2.5a$. The frequency spectra clearly show the logarithmic singularity at small frequencies. The vertical displacement for a static load is, in fact, logarithmic in r (Love, 1944) and can have an arbitrary additive constant. Therefore, for the purpose of plotting the frequency dependance of displacement amplitude, the zero frequency values correspond to $\omega a/\pi\beta = 0.005$. However, both synthetics and results in the frequency domain, for $\omega a/\pi\beta > 1$ correctly describe the effects of topography upon the incidence of Rayleigh waves. This can be seen on the synthetics which show the appropriate amplitude of the incident wave.

Figures 4 and 5 display the responses of the

deep and shallow triangular canyons for incident P and SV waves with incidence angles of 30° and 45°, respectively. For the deep canyon large variations in both space and frequency plots can be seen. The synthetics show diffracted Rayleigh waves with a criss-cross pattern. For the shallow canyon the synthetics show minor effects. In fact, a small-amplitude Rayleigh wave is produced at the left rim. Frequency domain results also show large variations. In both cases, and for a wide range of frequencies, relative amplifications or de-amplifications are larger than 20. However, maximum amplification is of about 2.5 times the amplitude of the incoming wave. Sánchez-Sesma and Campillo (1991) studied other incidences and found that the absolute maximum of response is generally lower than about 4.

Figure 6 illustrates the surface motion of the deep semi-elliptical canyon for incident SV waves. Again, a great variability emerges as a consequence of the superposition of incoming and reflected–diffracted energy. In the synthetics, the first arrivals at the right flat part clearly show both a delay and a reduction of amplitude that indicates a shadow zone and, thus, diffraction. In the figure the reflected SV wave is clearly seen along the left canyon's wall. This wave precedes diffracted creeping Rayleigh waves that propagate along the canyon's surface. These waves are produced at the corners and bounce back and forth between them. Early and late emissions of diffracted Rayleigh phases are also clearly seen in the flat part of the model. Results near the left rim seem to confirm the theoretical prediction of null motion at the vertex of a quarter space under the incidence of a plane SV wave propagating
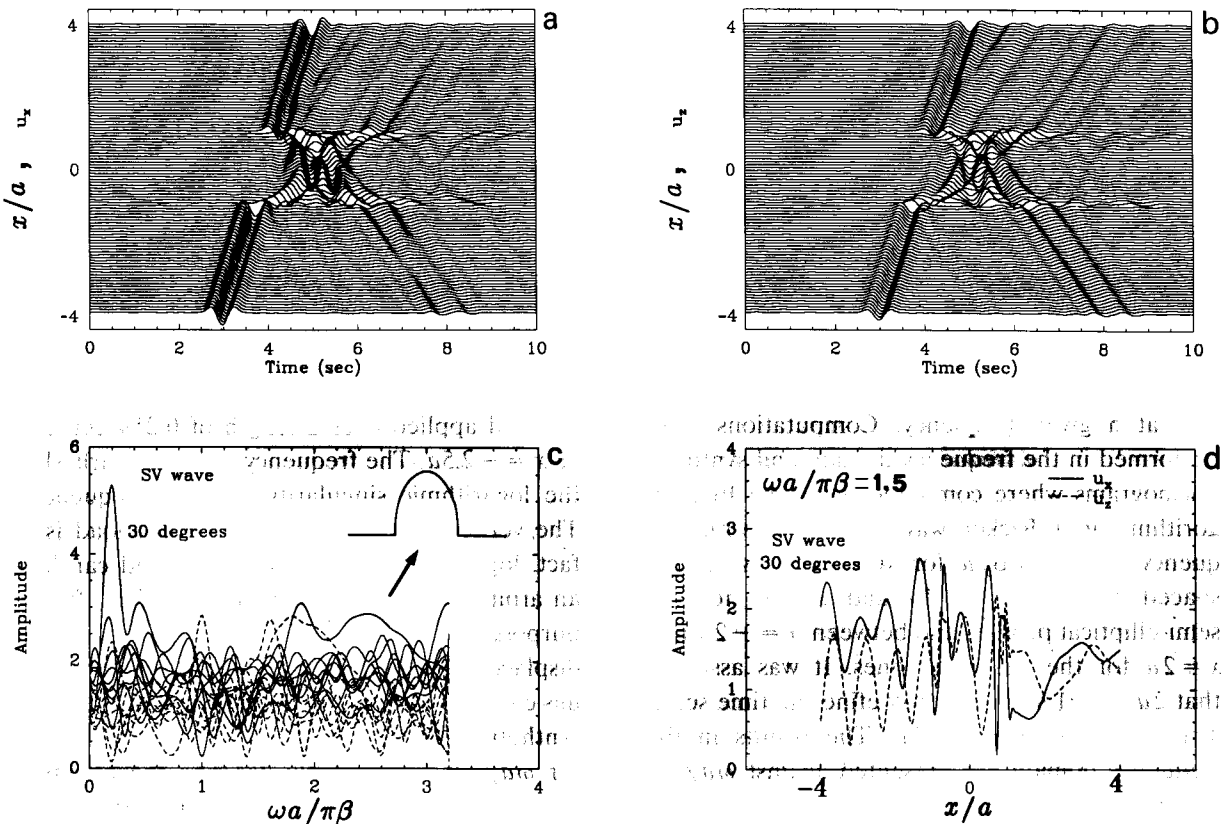

Fig. 7. Response to a nearby vertical load. Except at low frequencies, results correctly describe the effects of an incoming Rayleigh wave. Synthetic seismograms and frequency response for surface receivers equally spaced between $x = -2a$ and $x = 2a$ at the surface of a triangular mountain with unit slopes. (a)–(d) as in Fig. 4.

along the bisector angle (Sánchez-Sesma, 1990). The responses of the deep elliptical canyon to various types of incident waves show the appearance of creeping Rayleigh waves (see Sánchez-Sesma and Campillo, 1991).

Figure 7 shows a mountain with unit slopes under incident Rayleigh waves. Maximum amplifications do not exceed the level of 2 times the horizontal amplitude of the incident wave. As shown in the figure, the diffraction of Rayleigh waves mainly produces a backward-propagating phase of the same type. Figure 7c shows that the effect of the near-source terms of the applied load dominates at low frequencies.

In Figure 8 the surface motion of the semi-elliptical mountain for incident plane SV waves and 30° is illustrated. This is an extreme model that shows the wide potential applications of this approach. A great variability in the amplifications in the frequency domain is again present. At one receiver amplifications reach more than 5 times the amplitude of incident waves but the absolute level of amplification is, for this example, generally lower than about 3 times the amplitude of incoming waves. Time domain results show significant interference patterns, due to creeping waves along the curved part of the surface and the late emission of Rayleigh waves.

Conclusions

A method for computing the diffraction of P, SV and Rayleigh waves by an irregular topographic feature in an elastic half-space has been presented. It is based on a direct integral representation of the diffracted elastic fields in terms of single-layer boundary sources. A discretization scheme based on the numerical and analytical integration of exact Green's functions for displacements and tractions is employed. Our formulation can be seen as a numerical realization of Huygens' principle; that is, the diffracted waves are constructed at the boundary from which they are radiated. In addition to the physical insight gained with this method, it appears to be accurate and fast.

The results correspond to a relatively simple set of conditions, namely:

(1) the incidence of a plane wave (or the application of a vertical load in the neighborhood);

(2) the assumption of an elastic half-space with a Poisson ratio of $\frac{1}{4}$;

(3) a symmetrical shape for the irregularity.

Nevertheless, they display significant aspects of the response of topographic features. One of those is the spectacular amplitude of creeping waves and, as its counterpart, the large increase in the duration of the motion on the irregular topography.

Our results confirm the large variability of site effects, reported in the literature with respect to frequency, incidence angle and location of receivers. They show that variability is not restricted to the topographic feature: its presence strongly affects nearby locations. They also show that the interaction of elastic waves produce complex amplification and de-amplification patterns. For example, Bard and Tucker (1985) observed significant amplifications at some underground sites and concluded that they were due to free surface reflections. We believe that, despite the relative simplicity of our models, our results give a glimpse of the effects that the real topographic feature may induce. They present very large relative amplifications with values that, in many cases, can be larger than 20.

The plots of the frequency response at various locations show why simple spectral ratios cannot account for the seismic behavior of topographies. The large variability in the spectral content of ground motion in both frequency and space suggests that, in order to interpret the data, we cannot rule out the need for a quantitative model and careful assessment of the type of incoming waves as well. Therefore, the selection of reference sites and the windowing of the records are crucial for characterizing topographical effects by means of spectral ratios. For windowing data, a polarization analysis, such as that of Bernard and Zollo (1989), can be useful. In any event, our results (those shown here and in Sánchez-Sesma and Campillo (1991)) show that the absolute level of amplification is generally lower than about 4 times the amplitude of incoming waves.

Acknowledgements

Thanks are given to M. Bonnet for his comments and suggestions, to D.A. Alvarez-Cuevas and J. Ramos-Martínez for the critical reading of the manuscript, and to M. Suarez for her assistance. K. Aki, P.-Y. Bard, M. Bouchon, V. Farra, R. Madariaga and A. Wirgin made valuable suggestions. The critical comments from two anonymous reviewers helped to improve this work. Part of this study was carried out while one of us (F.J.S.-S.) was on leave from the National University of Mexico and the Centro de Investigacion Sísmica A.C., Mexico, at the Université Joseph Fourier of Grenoble, France, and Laboratoire de Sismologie of the Institute de Physique du Globe of Paris, France, as a Visiting Professor. Some computations were performed at Centre de Calcul Vectoriel pour la Recherche. This work was partially supported by Pole Grenoblois de Recherche sur les Risques Naturels, University of Paris VI, France, by Departamento del Distrito Federal, Mexico, and by Consejo Nacional de Ciencia y Tecnología, Mexico, under Grants P127CCOT904892 and P0523-T9109.

References

Abramowitz, M. and Stegun, I.A., 1972. Handbook of Mathematical Functions. Dover, New York.
Aki, K., 1988. Local site effects on strong ground motion. In: J.L. Von Thun (Editor), Earthquake Engineering and Soil Dynamics II—Recent advances in ground motion evaluation. (Geotechnical Spec. Publ. No. 20.) Am. Soc. Civil Eng., New York, pp. 103–155.
Bard, P.-Y., 1982. Diffracted waves and displacement field over two-dimensional elevated topographies. Geophys. J.R. Astron. Soc., 71: 731–760.
Bard, P.-Y. and Tucker, B.E., 1985. Underground and ridge site effects: a comparison of observation and theory. Bull. Seismol. Soc. Am., 75: 905–922.
Bernard, P. and Zollo, A., 1989. Inversion of near-source S polarization for parameters of double-couple point sources. Bull. Seismol. Soc. Am., 79: 1779–1809.
Bonnet, M., 1986. Méthode des equationes integrales regularisees en elastodynamique. PhD Thesis, Ecole Nat. Ponts et Chaussees, Paris.
Bonnet, M., 1989. Regular boundary integral equations for three-dimensional finite or infinite bodies with and without curved cracks in elastodynamics. In: C.A. Brebbia and

N.G. Zamani (Editors), Boundary Element Techniques: Applications in Engineering. Computational Mechanics, Southampton.
Bouchon, M., 1973. Effect of topography on surface motion. Bull. Seismol. Soc. Am., 63: 615–632.
Bouchon, M., 1979. Discrete wave number representation of elastic wave fields in three-space dimensions. J. Geophys. Res., 84 (B7): 3609–3614.
Bouchon, M., 1985. A simple, complete numerical solution to the problem of diffraction of SH waves by an irregular surface. J. Acoust. Soc. Am., 77: 1–5.
Bouchon, M. and Aki, K., 1977. Discrete wave-number representation of seismic-source wave fields. Bull. Seismol. Soc. Am., 67: 259–277.
Bouchon, M., Campillo, M. and Gaffet, S., 1989. A boundary integral equation—discrete wavenumber representation method to study wave propagation in multilayered media having irregular interfaces. Geophysics, 54: 1134–1140.
Campillo, M., 1987. Modeling of SH wave propagation in an irregularly layered medium. Application to seismic profiles near a dome. Geophys. Prospect., 35: 236–249.
Campillo, M. and Bouchon, M., 1985. Synthetic SH seismograms in a laterally varying medium by the discrete wavenumber method. Geophys. J.R. Astron. Soc., 83: 307–317.
Campillo, M., Sánchez-Sesma, F.J. and Aki, K., 1990. Influence of small lateral variations of a soft surficial layer on seismic ground motion. Int. J. Soil Dyn. Earthquake Eng., 9: 284–287.
Davis, L.L. and West, L.R., 1973. Observed effects of topography on ground motion. Bull. Seismol. Soc. Am., 63: 283–298.
Dravinski, M., 1982. Influence of interface depth upon strong ground motion. Bull. Seismol. Soc. Am., 72: 597–614.
Dravinski, M. and Mossessian, T.K., 1987. Scattering of plane harmonic P, SV and Rayleigh waves by dipping layers of arbitrary shape. Bull. Seismol. Soc. Am., 77: 212–235.
Gaffet, S. and Bouchon, M., 1989. Effects of two-dimensional topographies using the discrete wavenumber–boundary integral equation method in P–SV cases. J. Acoust. Soc. Am., 85: 2277–2283.
Geli, L., P.-Y. Bard and Jullien, B., 1988. The effect of topography on earthquake ground motion: A review and new results. Bull. Seismol. Soc. Am., 78: 42–63.
Griffiths, D.W. and Bollinger, G.A., 1979. The effect of Appalachian mountain topography on seismic waves. Bull. Seismol. Soc. Am., 69: 1081–1105.
Kawase, H., 1988. Time–domain response of a semicircular canyon for incident SV, P, and Rayleigh waves calculated by the discrete wavenumber boundary element method. Bull. Seismol. Soc. Am., 78: 1415–1437.
Kawase, H. and Aki, K., 1989. A study on the response of a soft basin for incident S, P and Rayleigh waves with special reference to the long duration observed in Mexico City. Bull. Seismol. Soc. Am., 79: 1361–1382.
Kelly, K.R. and Marfurt, K.J., 1990. Numerical modeling of

seismic wave propagation. (Geophysics Reprint Series, No. 13.) Soc. Explor. Geophys., Tulsa, Okla., USA.

Kobayashi, S., 1987. Elastodynamics. In: D.E. Beskos (Editor), Boundary Element Methods in Mechanics. North-Holland, Amsterdam.

Kupradze, V.D., 1963. Dynamical problems in elasticity. In: I.N. Sneddon and R. Hill (Editors), Progress in Solid Mechanics, Vol. III. North-Holland, Amsterdam, pp. 191–255.

Lamb, H., 1904. On the propagation of tremors over the surface of an elastic solid. Philos. Trans. R. Soc. London Ser. A, 203: 1–42.

Lee, V.W. and Cao, H., 1989. Diffraction of SV waves by circular canyons of various depths. J. Eng. Mech. Am. Soc. Civil Eng., 115: 2035–2056.

Love, A.E.H., 1944. A Treatise on the Mathematical Theory of Elasticity. Dover, New York.

Luco, J.E, Wong, H.L. and De Barros, F.C.P., 1990. Three-dimensional response of a cylindrical canyon in a layered half-space. Int. J. Earthquake Eng. Struct. Dyn., 19: 799–817.

Manolis, G.D and Beskos, D.E., 1988. Boundary Element Methods in Elastodynamics. Unwin Hyman, London.

Sánchez-Sesma, F.J., 1987. Site effects on strong ground motion. Int. J. Soil Dyn. Earthquake Eng., 6: 124–132.

Sánchez-Sesma, F.J., 1990. Elementary solutions for the response of a wedge-shaped medium to incident SH and SV waves. Bull. Seismol. Soc. Am., 80: 737–742.

Sánchez-Sesma, F.J. and Campillo, M., 1991. Diffraction of P, SV and Rayleigh waves by topographical features: a boundary integral formulation. Bull. Seismol. Soc. Am., 81: 2234–2253.

Sánchez-Sesma, F.J. and Esquivel, J., 1979. Ground motion on alluvial valleys under incident plane SH waves. Bull. Seismol. Soc. Am., 69: 1107–1120.

Sánchez-Sesma, F.J. and Rosenblueth, E., 1979. Ground motion at canyons of arbitrary shape under incident SH waves. Int. J. Earthquake Eng. Struct. Dyn., 7: 441–450.

Sánchez-Sesma, F.J., Bravo, M.A. and Herrera, I., 1985. Sur-face motion of topographical irregularities for incident P, SV and Rayleigh waves. Bull. Seismol. Soc. Am., 75: 263–269.

Todorovska, M.I. and Lee, V.W., 1992a. Surface motion of shallow circular alluvial valleys for incident plane SH waves—analytical solution. Int. J. Soil Dyn. Earthquake Eng. (in press).

Todorovska, M.I. and Lee, V.W., 1992b. A note on response of shallow circular valleys to Rayleigh waves—analytical approach. Earthquake Eng. Eng. Vibration (in press).

Trifunac, M.D., 1971. Surface motion of a semi-cylindrical alluvial valley for incident plane SH waves. Bull. Seismol. Soc. Am., 61: 1755–1770.

Trifunac, M.D., 1973. Scattering of plane SH waves by a semi-cylindrical canyon. Int. J. Earthquake Eng. Struct. Dyn., 1: 267–281.

Trifunac, M.D. and Hudson, D.E., 1971. Analysis of the Pacoima Dam accelerogram. San Fernando, California, earthquake of 1971. Bull. Seismol. Soc. Am., 61: 1393–1411.

Tucker, B.E., King, J.L., Hatzfeld, D. and Nersesov, I.L., 1984. Observations of hard-rock site effects. Bull. Seismol. Soc. Am., 74: 121–136.

Wong, H.L., 1979. Diffraction of P, SV and Rayleigh waves by surface topographies. Dep. Civil Eng. Univ. Southern California, Los Angeles, Calif., Rep. CE 79-05.

Wong, H.L., 1982. Effect of surface topography on the diffraction of P, SV and Rayleigh waves. Bull. Seismol. Soc. Am., 72: 1167–1183.

Wong, H.L. and Jennings, P.C., 1975. Effect of canyon topographies on strong ground motion. Bull. Seismol. Soc. Am., 65: 1239–1257.

Woods, R.D., 1968. Screening of surface waves in soils. J. Soil Mech. Found. Div. Am. Soc. Civil Eng., 94: 951–979.

Zhang, L. and Chopra, A.K., 1991. Three-dimensional analysis of spatially varying ground motions around a uniform canyon in a homogeneous half-space. Int. J. Earthquake Eng. Struct. Dyn., 20: 911–926.